International Conference on Applied Energy 2019
Aug 12-15, 2019, Västerås, Sweden
Paper ID: 0157

Two-level Energy Harvesting Strategy for Parallel Automotive Exhaust Thermoelectric Generator

Xiaolong Li[1,2], Changjun Xie[1,*], Shuhai Quan[1,2]

1 School of Automation, Wuhan University of Technology, Wuhan 430070, China

2 Hubei Key Laboratory of Advanced Technology for Automotive Components, Wuhan 430070, China

ABSTRACT

An automotive exhaust thermoelectric generator (AETEG) has a non-uniform temperature field among thermoelectric modules (TEMs), resulting in current mismatches of TEMs and lower energy output of the AETEG. In order to implement high maximum power point tracking efficiency of the AETEG, a distributed thermoelectric energy recovery system consisting of three parallel thermoelectric generators and lithium iron phosphate ($LiFePO_4$) battery pack is proposed. In addition, a two-level energy harvesting strategy is developed to efficiently recover more automotive exhaust energy, and guarantee the safety of the proposed system under the modified Highway Fuel Economy Test (HWFET) driving cycle. The proposed strategy aims to achieve the lower power loss of DC/DC converters and keep the battery pack working at the optimal point. When the initial SOC of $LiFePO_4$ battery pack is 10%, the charging energy has been increased by 174013J and the efficiency of DC/DC converters has been raised of 2.4% than PI control.

Keywords: automotive exhaust thermoelectric generator, parallel thermoelectric generator, two-level energy harvesting strategy, power loss

1. INTRODUCTION

Energy security and environmental issues have drawn great attentions to the energy consumption and environment deterioration, especially related to automotive exhaust emissions. According to the literature review [1], approximately 1/3 of the energy produced by the automotive fuel is consumed as waste heat through the exhaust gas. The automotive exhaust thermoelectric generator (AETEG) is proposed as the most promising technology for energy reuse in vehicles.

An AETEG consists of a certain number of thermoelectric modules (TEMs), arranged in an electric topology. Compared with the traditional centralized conversion architecture [2], the proposed distributed power converter, in which each thermoelectric module connects with a converter separately, has three advantages [3]. In order to regulate the voltage from the unregulated AETEG source, DC/DC converters embedded in maximum power point tracking (MPPT) algorithm and manage battery charging are applied in the AETEG application. Gao et al. [4] designed a combined control scheme with an MPPT before the battery is fully charged and a constant voltage for floating charge. Kim et al. [5] proposed a seamless mode transfer MPPT controller, including two different modes: the MPPT mode and power balance mode. Wu et al. [6] employed a control method to ensure smooth switching among different working modes. The problem with previous literatures is they do not consider the DC/DC converters' power loss.

In this paper, a two-level energy harvesting strategy is developed to guarantee the safety operation of the proposed system. The proposed control architecture consists of two levels: device control level and system control level. At the device control level, the AETEG works at two modes: MPPT mode and constant current mode; and the battery is controlled by droop method, making the AETEG and battery work at maximum power point and optimal charging state, respectively. At the system level, the proposed energy harvesting strategy incorporates equivalent generation maximizing strategy and dynamic programming to minimize the power loss of DC/DC converters.

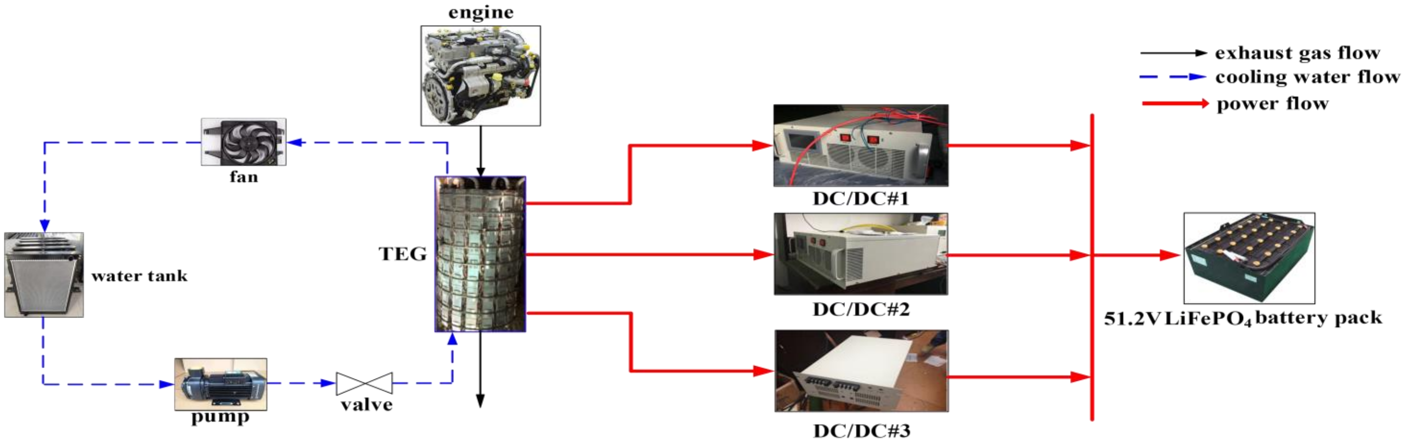

Fig 1 Schematic of distributed thermoelectric energy recovery system

2. SYSTEM MODEL DESCRIPTION

The proposed system is shown in Figure 1, which consists of a TEG and a 51.2V, 60Ah $LiFePO_4$ battery pack connected by three Sepic DC/DC converters in parallel. In the proposed system, the TEG power output and the charging current of the battery are coordinated approximately by controlling three DC/DC converters.

2.1 AETEG model

The shape of the AETEG is an eighteen-sided polygon prism and 306 TEMs are distributed into 17 rows in the streamwise direction and 18 columns located in the plane perpendicular to the heat flow. From the direction of exhaust inlet, TEMs from the 1st row to the 7th row, the 8th row to the 12th row, the 13th row to the 17th row belong to the high, medium, low temperature region, respectively. For one TEM, the performance parameters are listed in Table 1.

Table 1 Performance parameters of TEM

Parameter	Value
dimensions (L·W·H, mm)	50×50×4.2
weight (g)	47
maximum power (W)/hot, cold-side	14.0/250,
temperature (℃)	30
conversion efficiency (%)	5.6
material	Bi_2Te_3
manufacturer	GuangDong Fuxin

The open-circuit voltage $U_{OC\text{-}H}$, $U_{OC\text{-}M}$, $U_{OC\text{-}L}$, internal resistance $R_{TEG\text{-}H}$, $R_{TEG\text{-}M}$, $R_{TEG\text{-}L}$ of the high, medium, low temperature region of AETEG, Seebeck coefficient, electrical resistivity of thermoelectric material in the row ith (1≤i≤17) TEMs are given by the following expressions:

$$U_{OC\text{-}H}=\sum_{i=1}^{7} N\cdot\alpha_{PNi}\cdot\Delta T_i \tag{1}$$

$$R_{TEG\text{-}H}=\sum_{i=1}^{7}(N/18)\cdot\rho_{PNi}\cdot(L/S) \tag{2}$$

$$U_{OC\text{-}M}=\sum_{i=8}^{12} N\cdot\alpha_{PNi}\cdot\Delta T_i \tag{3}$$

$$R_{TEG\text{-}M}=\sum_{i=8}^{12}(N/18)\cdot\rho_{PNi}\cdot(L/S) \tag{4}$$

$$U_{OC\text{-}L}=\sum_{i=13}^{17} N\cdot\alpha_{PNi}\cdot\Delta T_i \tag{5}$$

$$R_{TEG\text{-}L}=\sum_{i=13}^{17}(N/18)\cdot\rho_{PNi}\cdot(L/S) \tag{6}$$

where N is the number of PN junctions in each TEM; ΔT_i is the temperature difference between hot sides and cold sides of TEMs in the ith row; T_{mi} is the half of the ΔT_i; L is the length of the thermoelements, and S is the cross section area of one pair of PN junctions. Then, the maximum output power of the high, medium, low temperature region of AETEG model is derived by Thevenin theorem.

2.2 $LiFePO_4$ battery pack model

The $LiFePO_4$ battery pack consists of 16 single batteries connected in series rated 51.2V, 45Ah. The behavior of the battery is represented by the effective internal resistance battery model, which does not consider the impact of temperature change and battery aging. Therefore, the battery SOC and output current are described as follows:

$$SOC=SOC_{t0}-\frac{1}{Q_b}\int_{t0}^{t} I_{bat}(t)dt \tag{7}$$

$$I_{bat}=\frac{V_{oc}-\sqrt{V_{oc}^2-4R_{int}\cdot P_{bat}}}{2R_{int}} \tag{8}$$

where SOC_{t0} is the SOC at time index t0, V_{oc}, R_{int}, P_{bat}, I_{bat} and Q_b are the open-circuit voltage, internal resistance, output power, output current, maximum capacity of battery, respectively.

2.3 Sepic DC/DC converter model

To interface with the AETEG which has a wide output voltage range, the Sepic DC/DC converter is adopted to meet the power demand of the battery pack in this system. The efficiency of the converter is calculated as:

$$\eta=\frac{P_{out}}{P_{in}}=\frac{P_{out}}{P_{out}+P_{switch}+P_{conduction}} \tag{9}$$

where, P_{in} is the input power, P_{out}= V_o I_o is the output power, P_{switch} is the switching loss of the power device, $P_{conduction}$ is the current loss, including the voltage drop loss of the diode and the loss of various resistors.

According to Sepic converter circuit simulation data and curve fitting tool in Matlab software, the efficiency curve of three Sepic converters shown in Figure 2 could be acquired. Since sum of squared errors of data points in converter 1, 2, 3 is 0.0008767, 0.003651, 0.0001194, respectively, the efficiency curve fitted by the efficiency function is approximately close to the simulation data.

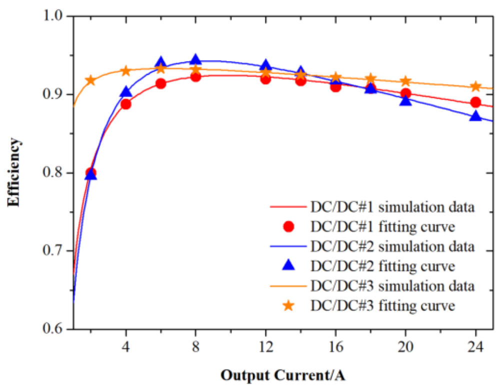

Fig 2 Efficiency curves of three Sepic converters

3. TWO-LEVEL ENERGY HARVESTING STRATEGY

3.1 Control objectives

The energy harvesting strategy should fulfill the following control objectives:

(a)To ensure that the AETEG works at the MPPT point as often as possible;

(b)To minimize the DC/DC converter loss and improve the system efficiency;

(c)To maintain the SOC of the $LiFePO_4$ battery pack within an efficient region;

(d)To enhance the battery life by keeping the $LiFePO_4$ battery pack working at the optimal point as much as possible.

3.2 Device control level

3.2.1 AETEG

The AETEG has two working modes under different operating states: MPPT mode, and current mode. The AETEG works mostly in the MPPT mode to recycle waste heat energy as much as possible; however, it will switch to the current mode when the SOC of $LiFePO_4$ battery pack is close to the maximum SOC (SOC_{max}) or its output power is higher than the limit.

3.2.2 $LiFePO_4$ battery pack

The droop control method is used to figure out the optimal power demand of $LiFePO_4$ battery pack and to maintain the SOC of $LiFePO_4$ battery pack in an efficient range. And it can be expressed as:

$$P_{batopt}=P_H - mI_b \quad I_b<0,\text{charging} \tag{10}$$

where, P_{batopt} is the optimal power demand of $LiFePO_4$ battery pack, P_H is the critical power value of charging, I_b is the output current of battery pack, m is the adaptive droop coefficient.

3.3 System control level

3.3.1 Equivalent generation maximizing strategy

EGMS is an instantaneously optimized approach which can maximize the charging power of battery. In order to maximize the charging power of battery, the AETEG is in the MPPT mode to recycle waste heat energy as much as possible. And the maximizing problem of the charging power can be formulated as:

$$J_1=\text{argmax}\sum_{i=1}^{3} P_{TEG\text{-}i}\cdot\eta_i$$

$$\text{s.t.}\ \begin{cases} SOC_{min}\le SOC\le SOC_{nom} \\ I_{oimin}\le I_{oi}\le I_{oimax} \end{cases} \tag{11}$$

where, $P_{TEG\text{-}i}$ (i=1,2,3) are the maximum output power of AETEG high, medium, low temperature region; accordingly, η_i (i=1,2,3) are the efficiency of Sepic DC/DC#i (i=1,2,3). This optimization problem is subject to the constraints: SOC_{min} and SOC_{nom} are the lower limit and upper threshold of $LiFePO_4$ battery pack SOC in the normal level; I_{oimin} and I_{oimax} are the minimum and maximum output current of the i^{th} Sepic converter.

3.3.2 Dynamic programming

Dynamic programming (DP) is used to improve the recovery efficiency while keeping the $LiFePO_4$ battery pack working at the optimal point. Since the efficiency of the power system is determined by the output current of the i^{th} (i=1, 2, 3) Sepic converter directly, it is selected as the system objective function. The change of the battery SOC describes the dynamic process of the battery; therefore, the battery SOC is selected as the state variable of the system. Because the output current of the i^{th} (i=1, 2, 3) Sepic converter is related to each other, they are selected as decision variables.

4. RESULTS AND DISCUSSIONS

The proposed energy harvesting strategy combined with AETEG energy recovery system is verified in simulation test. The modified 4590 s HWFET driving cycle is chosen as the test driving cycle and the initial SOC of battery is 10%, 40%，and 70%, respectively. The results are shown in Figure 3.

Figure 3 shows results of modified HWFET driving cycle, including the instantaneous output current of three Sepic converters and SOC of the $LiFePO_4$ battery, which can reflect the control performance of the proposed two-level energy harvesting strategy under three initial SOCs of the $LiFePO_4$ battery. In case 1, the SOC of the $LiFePO_4$ battery pack increases rapidly from 10 to 63.01%. In case 2, the battery's SOC rises dramatically to 80.11%. In case 3, the fluctuation range of the SOC of the $LiFePO_4$ battery pack is 22.51%. Therefore, the proposed strategy is proved to be valid.

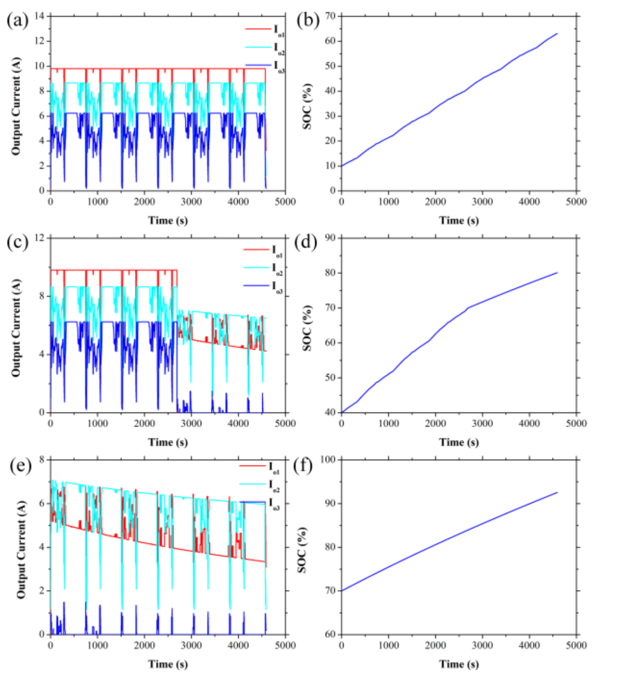

Fig 3 The output currents of Sepic converters (a)$SOC_{initial}$=10%; (c)$SOC_{initial}$=40%; (e)$SOC_{initial}$=70%; The charging curve of battery's SOC (b)$SOC_{initial}$=10%; (d)$SOC_{initial}$=40%; (f)$SOC_{initial}$=70%.

The comparisons of the proposed two-level energy harvesting strategy and PI-based control strategy are summarized in Table 2.

Table 2 The comparison of control performance

Initial SOC	$\eta_{con,avg}$		E_{chg}	
	PI	Two-level	PI	Two-level
10%	90.39%	92.79%	6553740J	6727753J
40%	92.15%	93.71%	4900493J	4983454J
70%	93.82%	94.19%	2863195J	2874487J

From Table 2, compared with the classical PI control strategy (93.82%), the proposed two-level energy harvesting strategy shows a better operating economy, which has the highest average efficiency of DC/DC converters (94.19%) when the initial SOC of battery is 70%.Whether the initial SOC of $LiFePO_4$ is 10%, 40%, 70%, charging energy of battery based on the classical PI control strategy (6553740J, 4900493J, 2863195J)are less than the proposed two-level energy harvesting strategy's (6727753J, 4983454J, 2874487J).

5. CONCLUSIONS

In this paper, a distributed thermoelectric energy recovery system consisting of an AETEG and a $LiFePO_4$ battery pack is developed. Different distributed devices composing this proposed system have been modeled to take system dynamics into account. Then, a two-level energy harvesting strategy is proposed for the distributed thermoelectric energy recovery system. The proposed energy harvesting strategy containing the device and system control level is responsible for achieving the lowest loss of DC/DC converters, keeping the battery working at the optimal point, and making full use of the AETEG energy. According to simulation results, two-level energy harvesting strategy is more suitable for the proposed system.

ACKNOWLEDGEMENT

This work was supported in part by the National Natural Science Foundation of China (51477125), in part by the Hubei Science Fund for Distinguished Young Scholars (2017CFA049), and in part by the Hubei province technological innovation major project (2018AAA059).

REFERENCE

[1] Patowary R, Baruah DC. Thermoelectric conversion of waste heat from IC engine-driven vehicles: A review of its application, issues, and solutions. Int J Energ Res 2018;42(8):2595–2614.
[2] Yu C, Chau KT. Thermoelectric automotive waste heat energy recovery using maximum power point tracking. Energ Convers Manage 2009;50(6):1506-12.
[3] Li ML, Xu SH, Chen Q, et al. Thermoelectric-generated-based DC-DC conversion networks for automotive applications. J Electron Mater 2011; 40(5):1136-43.
[4] Gao JL, Sun K, Ni LX, et al. A thermoelectric generation system and its power electronics stage. J Electron Mater 2012; 41(6):1043-50.
[5] Kim RY, Lai JS. A seamless mode transfer maximum power point tracking controller for thermoelectric generator applications. IEEE T Power Electr 2008; 23:2310-18.
[6] Hu HF, Sun K, Zhang JJ, et al. A TEG efficiency booster with Buck-Boost conversion. J Electron Mater 2013; 42(7):1737-44.